analytical chemistry

Article

pubs.acs.org/ac

General, Label-Free Method for Determining K_d and Ligand Concentration Simultaneously

Farzad Jalali-Yazdi,[†] Terry T. Takahashi,[‡] and Richard W. Roberts*[,†,‡,§,∥]

[†]Mork Family Department of Chemical Engineering and Materials Science, [‡]Department of Chemistry, [§]Department of Molecular Computational Biology, and [∥]USC Norris Comprehensive Cancer Center, University of Southern California, Los Angeles, California 90089-2905, United States

Supporting Information

ABSTRACT: Some of the most commonly used affinity reagents (e.g., antibodies) are often developed and used in conditions where their input concentrations ($[L]_0$) and affinities (K_d) are not known. Here, we have developed a general approach to determine both $[L]_0$ and K_d values simultaneously for affinity reagents (small molecules, proteins, and antibodies). To do this, we perform quantitative equilibrium exclusion immunoassays with two different concentrations of target and fit the data simultaneously to determine K_d and $[L]_0$. The results give accurate and reproducible measures of both values compared to established methods. By performing detailed error analysis, we demonstrate that our fitting gives unique solutions and indicates where K_d and $[L]_0$ measures are reliable. Furthermore, we found that a divalent model of antibody binding gives accurate K_d and $[L]_0$ values in both the forward (antibody immobilized) and the reverse (target immobilized) assays—addressing the long-term problem of obtaining quantitative data from reverse assays.

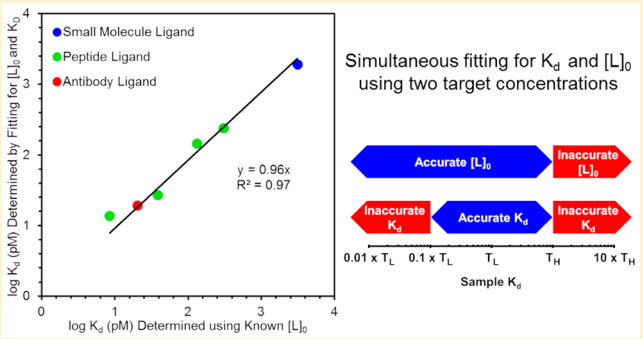

Immune assays remain the most widely used method for protein detection, tracking, and characterization. The generation of proteome-wide immune reagents provides an important route to address cancer biology, immunology, and basic research. However, a problem with most antibody-based assays is that neither the antibody concentration ($[L]_0$) nor the affinity (K_d) for the target is generally known.[1−3] This is suboptimal in a variety of important situations, ranging from antibody screening to quantitative immunoassays, and in the development of therapeutic antibodies, where efficacy directly relates to affinity and specificity.[4]

Generally, it is assumed that in order to determine K_d for a ligand−protein interaction, one must know the concentration of the ligand. In this view, titration of the ligand with a target over a concentration range, combined with a method for detecting the ligand−target complex, provides a direct means to determine K_d values.[5,6] For this reason, quantitative analysis using antibody-based assays is difficult, since the concentration of the antibody is often unknown. A second issue with antibody-based diagnostics is that the prevailing model for analyzing equilibrium data treats antibodies as monovalent reagents.[7−9] This approach can work for the forward assay (target in solution) but produces erroneous results for the reverse assay (target immobilized).[10,11] A third major issue is that measuring K_d for high-affinity ligands can be challenging because long off-rates can bias results, while some indirect methods require chemical labeling of ligands, which can alter K_d.[12−14]

Here, we developed a general approach to determine both K_d and $[L]_0$ values simultaneously by fitting the data to the equilibrium model. To do this, we use a modified version of the equilibrium assay first developed by Friguet et al.[7] At the core of our work is the combination of simultaneous fitting of both parameters with data from two separate target concentrations. Modeling and error analysis of experimental and simulated data enable us to demonstrate that the method is accurate and further define conditions where our results are correct. Using our approach, we have analyzed and overcome a significant problem in the field: proper modeling and analysis of reverse assays.[10,11] Overall, our approach is platform-independent and can be used in any system where protein concentrations can be accurately determined. We have demonstrated our approach using two established methods of protein analysis—classical Enzyme-Linked Immunosorbant Assay (ELISA) and Acoustic Membrane MicroParticle (AMMP) technology—with three different classes of reagents: peptides, antibodies, and small molecule ligands.

MATERIALS AND METHODS

Target and Ligands Used. In our experiments, we used ligands directed against B-cell lymphoma extra-large (Bcl-x_L),

Received: August 10, 2015
Accepted: October 20, 2015
Published: October 20, 2015

DOI: 10.1021/acs.analchem.5b03069
Anal. Chem. 2015, 87, 11755−11762

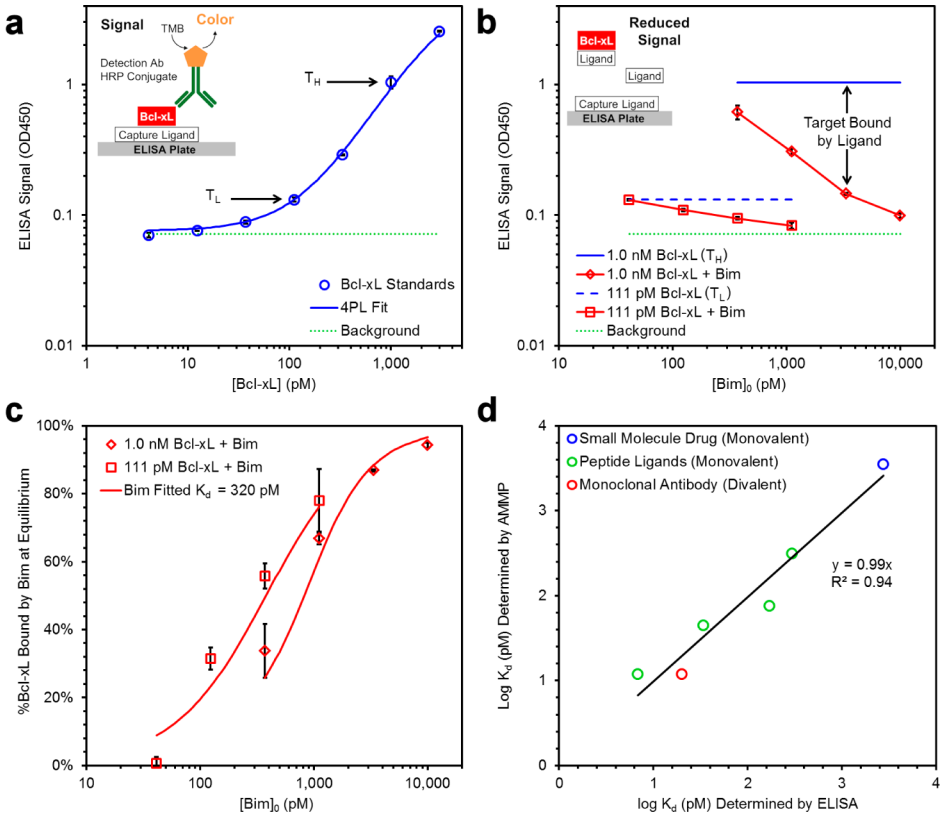

Figure 1. Measuring K_d via forward equilibrium immunoassays (target in solution). (a) The schematic and response curve for the ELISA. The Bcl-x_L signal is fit to a four-parameter logistic model. Two target concentrations were chosen for preincubation with Bim. (b) Loss of ELISA signal resulting from equilibrating 1 nM or 111 pM Bcl-x_L (red diamonds and squares, respectively) with Bim. The signal represents the unbound target (concentration calculated using data given in panel a). (c) Determining the K_d value for the ligand. The fraction of Bcl-x_L bound (%C_{EQ}, diamonds and squares) and ligand concentrations are fit to the equilibrium model (Supplementary Figures 1 and 2). Data from both high and low target concentrations are fit simultaneously to obtain a K_d value. (d) The K_d values obtained using a different platform for protein concentration measurement (the AMMP assay) are equivalent to the results obtained by ELISA for peptide, small-molecule, and antibody ligands.

which is an oncogenic protein that is up-regulated in several types of human carcinomas[15] and a target for therapeutic development. This protein has three distinct classes of known ligands: antibodies, peptides, and small molecules. We purchased two of these classes from commercial vendors: (1) monoclonal antibody 54H6 and (2) the high-affinity small molecule ABT-737.[16] For peptides, we synthesized a 26-residue fragment of Bim (a pro-apoptotic natural ligand of Bcl-x_L[17]) and three ultrahigh-affinity peptides ($K_d \leq 1$ nM) that bind to Bcl-x_L (Takahashi and Roberts, manuscript in preparation). Importantly for these assays, the peptides and small molecule bind one site in Bcl-x_L and the antibody binds a second, noncompeting site on the protein.

Monovalent and Divalent Analysis. The data for both sets of target concentrations were simultaneously fit for K_d (in the K_d-only fit) or K_d and $[L]_0$. The data are fitted to the equilibrium model using the lowest absolute deviation method, by varying either only K_d or both K_d and $[L]_0$ simultaneously. The monovalent assay fitting was done by Excel Solver (GRG Non-Lin method), using a set of five initial values. The set of values that provided the smallest error after the fitting were chosen as the final values. For the divalent assays, the fitting was performed using MATLAB's fminsearch function and a set of 10 initial values for K_{d1}, K_{d2}, and $[L]_0$. In order to calculate the %C_{EQ} value, first the concentration of monovalently bound antibody was found by determining the real, positive root of the cubic function in Supplementary Figure 2 in the Supporting Information. For the divalent reverse assay, an extra parameter (C_f) was also determined by fitting (see Reverse Assay in Supplementary Figure 2).

Simulated Error Analysis. To prepare the three-dimensional (3D) error plot in Figure 2d, we used eight simulated data points, where two $[T]_0$ values (T_H is high $[T]_0$ and T_L is low $[T]_0$, and $T_H = 10 \times T_L$) and four $[L]_0$ values were chosen (starting from $10 \times T_H$ diluted serially with a dilution factor of 1:10). We constructed a 2D matrix in MATLAB where the x-coordinate represents the deviation in K_d over a 2-order-of-magnitude window, and the y-coordinate represents the deviation in $[L]_0$. We then evaluated the total difference between %C_{EQ} when calculated using the deviated K_d and $[L]_0$ values, versus the true K_d and $[L]_0$ values for all eight data points, and dubbed this difference the error. The error matrix also is dependent on the relationship between the true K_d value and T_H. Six K_d/T_H ratios were tested, ranging from 100 to 0.01 (an example is shown in Figure 2d). These 2D error matrices were also used in the stepwise analysis for Supplementary Figure 3 in the Supporting Information. To perform this type of analysis, we chose a specific column (deviation in K_d) in the matrix. The row with the lowest error for the chosen column represents the optimum $[L]_0$ value for the specific deviation in K_d. If the initial chosen column also represents the lowest error in the optimum $[L]_0$ row, then the pair of K_d and $[L]_0$ are a stable pair. If not, then the lowest error in the row should be used to determine the new optimum deviation in K_d, and this

DOI: 10.1021/acs.analchem.5b03069
Anal. Chem. 2015, 87, 11755−11762

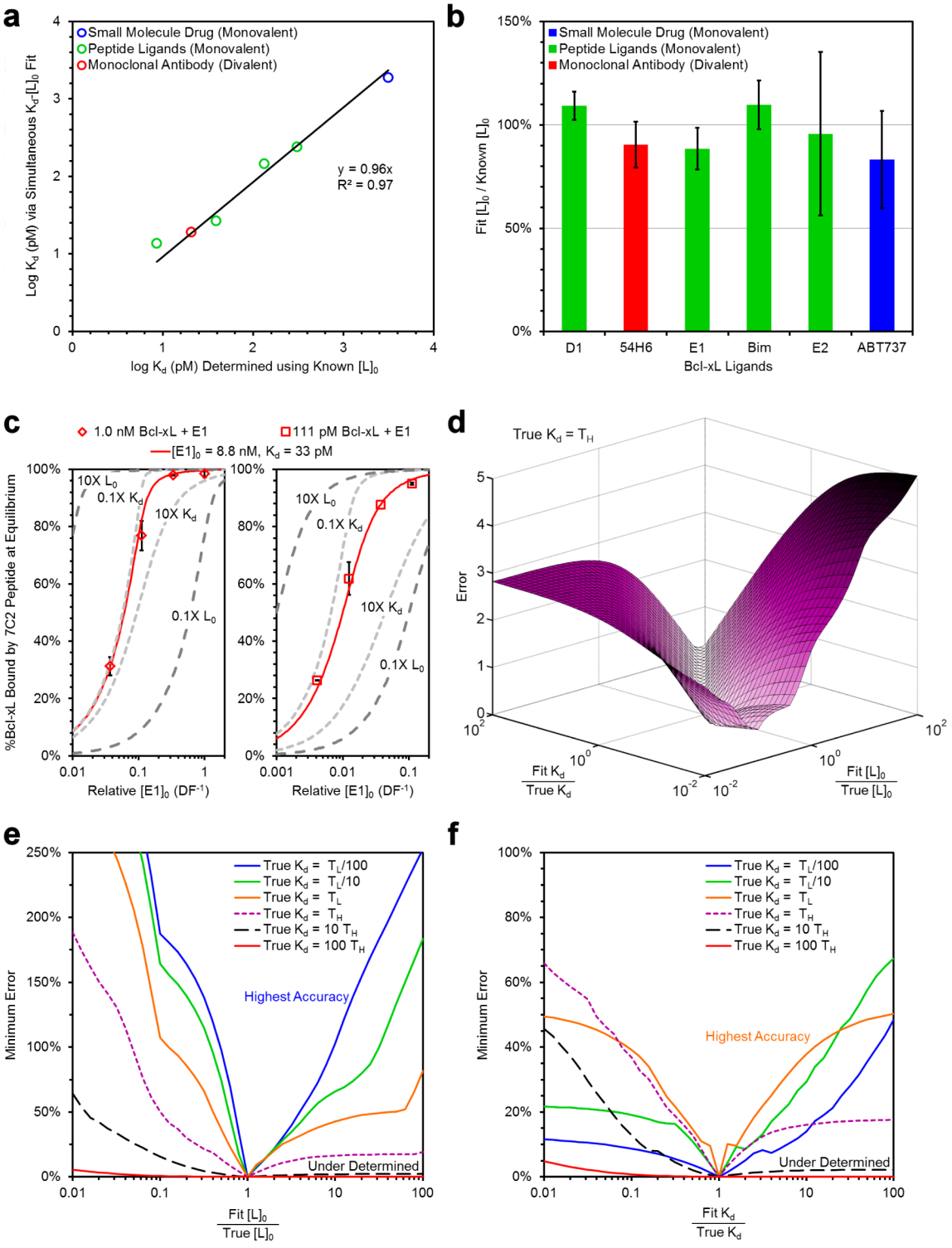

Figure 2. Simultaneous fitting of K_d and $[L]_0$ produces accurate results. (a) Fitting for K_d and $[L]_0$ simultaneously yields K_d values that are equivalent to the values obtained when $[L]_0$ is known. (b) Ligand concentrations determined by simultaneous fitting of K_d and $[L]_0$ match the known $[L]_0$. (c) Simultaneous fitting of K_d and $[L]_0$ for peptide E1 using the monovalent equilibrium model yields a unique solution (red line). Light gray and dark gray dashed lines demonstrate the fidelity of the fit to the high (T_H, red diamonds) and low (T_L, red squares) target concentration samples when K_d and $[L]_0$ are each varied ±10-fold while the other variable is held constant. Here, the *x*-axis is given as relative concentration (DF^{-1}) since $[L]_0$ is unknown. (d) Three-dimensional (3D) surface plot showing the error (absolute deviation, *z*-axis) between a simulated dataset calculated from true $[L]_0$ and K_d values, and datasets where $[L]_0$ and K_d are allowed to vary ±100-fold from their true values (see Materials and Methods). A unique and accurate solution for $[L]_0$ and K_d can be determined if the error surface only approaches the *x*–*y* plane at the true values of $[L]_0$ and K_d. (e, f) The lowest values of the projected error surface as viewed on the error vs $[L]_0$ or error vs K_d planes, respectively (details in Supplementary Figure 2). A higher error projection (e.g., the blue projection in panel c) corresponds to higher sensitivity of the measured parameter resulting in better accuracy and precision.

DOI: 10.1021/acs.analchem.5b03069
Anal. Chem. 2015, 87, 11755−11762

iterative method should be continued until a stable pair of values are obtained.

RESULTS AND DISCUSSION

Forward (Target in Solution) Equilibrium Assay. The forward assay refers to assays where the ligand (i.e., antibody) is used to capture the target from solution. The amount of target captured can be reduced, if the capture ligand binding epitope is blocked (by the capture ligand in solution or by a competing ligand). The forward assay is especially useful for screening multiple ligands to determine the best binding sequences that can block a specific interaction (e.g., generating therapeutic monoclonal antibodies), as it can rapidly determine the dissociation constants of multiple competing ligands for a single target. If all ligands bind to the same epitope, only a single capture ligand is needed to create a target response curve, greatly reducing the number of samples needed to accurately measure the K_d for all ligands. We used this feature to measure the K_d of multiple ligands with a single capture ligand and corresponding standard curve.

In order to determine the K_d for our ligands, we modified the method described by Friguet et al.[7] In this assay, a capture ligand pulls down the free target in solution. A competing ligand (of unknown K_d) is incubated with the target and allowed to equilibrate, reducing the amount of free target in solution. The K_d of interaction can then be determined by quantifying the amount of free target. The response curve for target quantitation and the schematic for the assay are shown in Figure 1a. Using the response curve, we chose two target concentrations that gave signal that was above background yet not saturated (111 pM and 1 nM, indicated with arrows) for our analysis. At each of these concentrations, competing ligand (Bim in Figure 1) was equilibrated with the sample to reduce the signal (Figure 1b). These data are fit to yield a single K_d and result in two curves that correspond to the different target concentrations (Figure 1c, equilibrium models are shown in Supplementary Figures 1 and 2).

This equilibrium assay is transferable to any method capable of sensitive measurement of analyte concentration. To show this, we used a commercially available quantitation platform, the ViBE BioAnalyzer, capable of high-throughput automatic sample analysis. Comparing the AMMP (ViBE Platform) and ELISA methods demonstrates that antibody, small-molecule, and peptide ligands give the same K_d values independent of the measurement method (slope of 0.99 and correlation coefficient of $R^2 = 0.94$; see Figure 1d and Supplementary Table 1 in the Supporting Information). This validates the AMMP approach for K_d measurements, because the accuracy of the equilibrium ELISA method has been shown extensively.[7] In addition, our measured K_d value for the Bim peptide (130 ± 40 pM) matches the reported value in the literature (140 pM).[18]

Measuring K_d in the Case of Unknown Ligand Concentration. Measuring the K_d by equilibrium assays or directly measuring the formation rate constant (e.g., by surface plasmon resonance) is very sensitive to the concentrations of target and ligand, and measuring the ligand concentration is not always simple. Many factors can complicate accurate measurement of ligand concentration, such as unknown expression levels, or unknown fraction of functional/correctly folded ligand, or the desire to use crude, unpurified samples for highest throughput.[19] This prerequisite is one issue that makes high-throughput K_d screens for ligands difficult, time-consuming, and infeasible on a proteomic scale.

The key insight of this work is in exploring whether K_d and $[L]_0$ can be determined simultaneously, and defining the conditions under which this analysis is accurate. In our experiments, to determine K_d values for Bcl-x_L ligands, we followed a traditional approach and determined the value of $[L]_0$ for each of our binders (Figure 1). We also reanalyzed this same data without inserting the value of $[L]_0$, and we attempted to determine both K_d and $[L]_0$ simultaneously.

This analysis revealed the same values of K_d (slope of 0.96 and $R^2 = 0.97$; see Figure 2a) and $[L]_0$ (<20% error; see Figure 2b) obtained using standard approaches for all three classes of ligands (values reported in Supplementary Table 2 in the Supporting Information). The correspondence between the two approaches is excellent, giving the same values of K_d over the entire range studied (from 8.5 pM to 3 nM). This might be possible in our work, compared to prior work in the field, because of the fact that we had used two sets of target concentrations to generate our equilibrium response curves, versus the more typical approach of using a single target concentration.

Fidelity of the Fit and Parameter Sensitivity. While the results from the simultaneous fit for K_d and $[L]_0$ look very promising, it is important to learn about the potential weaknesses of this type of analysis. We explored the sensitivity of our fitting to each of the input values of K_d and $[L]_0$. Figure 2c shows a rudimentary measure of the fidelity of each parameter. After obtaining K_d and $[L]_0$ values through simultaneous fitting, we kept one parameter constant and changed the other parameter by an order of magnitude in each direction to show the accuracy of the obtained values (indicated by light and dark gray dashed lines).

Plots of data similar to Figure 2c are often seen in the literature, as proof that the fit values for K_d and $[L]_0$ are correct.[20−24] When a pair of K_d and $[L]_0$ values are fit, the error between the data and the equilibrium model is plotted as one parameter being fixed, and the other being scanned over a range. Values are accepted when each parameter produces the minimum level of error when the other parameter is fixed (Supplementary Figures 3a and 3b in the Supporting Information). The shortcoming of this iterative fitting analysis is that it cannot show how changing one parameter can compensate for changing the other. This approach can result in self-consistent pairs of K_d and $[L]_0$ that are incorrect and far from the true K_d and $[L]_0$ values (see Supplementary Figure 3c).

Fitting for two variables simultaneously can result in a situation where varying one parameter can compensate for the error generated when the other parameter is moved. To address this problem, we carried out a more rigorous analysis of parameter sensitivity. To do this, we needed a way to visualize how the overall error changes for all combinations of fit K_d and $[L]_0$ values. Given the true K_d and $[L]_0$ values, and two target concentrations each with four dilutions of ligand, we simulated eight data points. We then varied K_d and $[L]_0$ within a 4-orders-of-magnitude window, and calculated binding percentages at equilibrium. Error was defined as the total distance between the two sets of data points (Figure 2d). This type of analysis produces an error surface where the z-axis corresponds to the error and the x- and y-axis values show the changes in K_d and $[L]_0$ using the true values of each as a reference point. Hence, at the center of the plot (where K_d and $[L]_0$ are equal to their true values), the error (z-axis) is defined as zero.

DOI: 10.1021/acs.analchem.5b03069
Anal. Chem. 2015, 87, 11755−11762

Looking at the plot in Figure 2d, it is clear that many different combinations of $[L]_0$ and K_d result in relatively large error values. Put another way, the error surface approaches the $x-y$ plane (where error is lowest) for a very restricted set of values of both parameters—the ravine running down the middle of the surface. This approach to viewing the data obscures whether there is a unique solution where error is minimized, or whether there are a family of solutions of K_d and $[L]_0$ that give error values very near the $x-y$ plane. To address this, we projected the error surface (Figure 2d) onto the $[L]_0$-error plane (Figure 2e) or the K_d-error plane (Figure 2f), and only retained the lowest error values for each projection (details shown in Supplementary Figure 4 in the Supporting Information). A point on each line in Figure 2e thus represents the minimum error for a given variation in $[L]_0$, over all tested K_d values. The lines corresponding to the error surface in Figure 2d can be seen as purple dashed lines in Figures 2e and 2f.

Viewed in this way, it becomes apparent that the accuracy of this analysis is dependent on the K_d value in relation to the concentrations of the target (low target concentration (T_L) and high target concentration (T_H)) used in the experiments. The purple dashed lines in Figures 2e and 2f produce a unique, unambiguous solution approaching the x-axis at a single point: the true value of $[L]_0$ and K_d, respectively. Some choices of target concentrations vs K_d can give even more clear solutions (blue, green, and orange curves in Figure 2e and the orange curve in Figure 2f). Importantly, there are choices of target concentrations that give ambiguous results (e.g., the red curve in Figure 2e and f). In these cases, it is clear that these target concentrations cannot be used to determine accurate values of K_d and $[L]_0$.

Indeed, this type of analysis can be formulated as a set of rules that direct where K_d and $[L]_0$ can be determined. When the high and low target concentrations are 10-fold apart and the ligand concentration ranges from $10 \times T_H$ to $0.1 \times T_L$, accurate K_d values can be obtained for $T_H > K_d > 0.1 \times T_L$. The accuracy of fit $[L]_0$ follows significantly different rules: the fit for $[L]_0$ is accurate when $T_H > K_d$, and it is improved continuously as K_d is lowered, with respect to initial target concentration. These ranges are guidelines for assessing the accuracy of the obtained K_d and $[L]_0$ values. If the obtained K_d value is within the $T_H > K_d > 0.1 \times T_L$ range, the fits can be trusted. However, if the obtained K_d is outside the window, the experiment must be repeated with new initial target concentrations. This same type of analysis can be used to demonstrate that accurate K_d and $[L]_0$ values cannot be determined using a single target concentration (see Supplementary Figure 5 in the Supporting Information), showing that at least two concentrations of target are needed.

The validity of the above ranges is shown in Figure 3. When the true K_d value is within the optimum range, a 5-fold deviation in fit K_d cannot be compensated for by adjusting the $[L]_0$ value (Figure 3a). Here, the erroneous K_d and $[L]_0$ values do not fit the data. However, if a single target concentration is used (Figure 3b), or K_d is outside the specified range (Figures 3c and 3d), the data points and the erroneous K_d and $[L]_0$ values match and would be falsely interpreted as "correct" K_d and $[L]_0$ values.

There are examples in the literature where others have worked to determine K_d and activity or K_d and $[L]_0$ iteratively. Our work indicates that these approaches are flawed, because they either use a single target concentration[22,24] or target concentrations outside of the window of accuracy.[20] Importantly, those analyses do not specify the ranges where the calculations are valid. Our results demonstrate that these approaches are prone to generate erroneous data while giving no indication that the fits are incorrect.

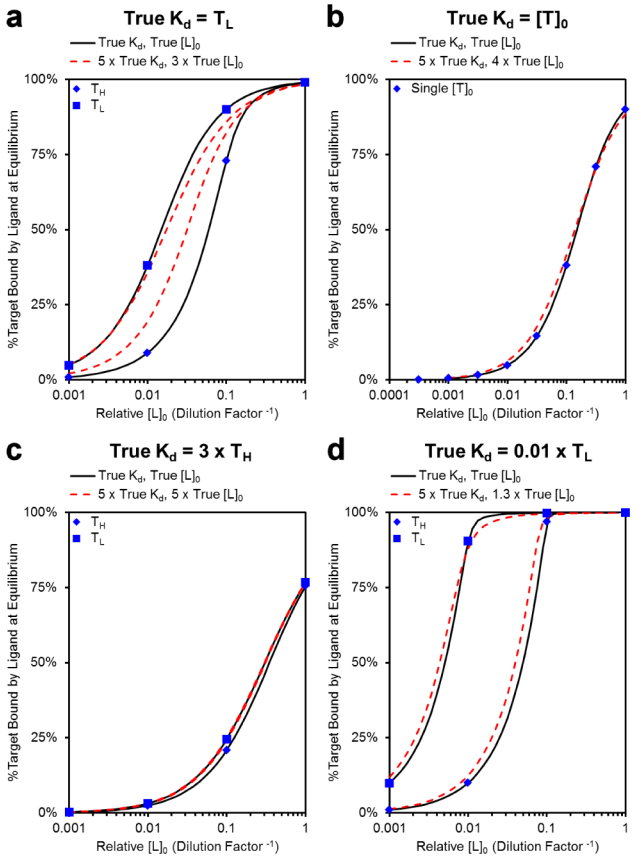

Figure 3. Fitting using two or more target concentrations that bracket K_d is required to derive accurate values for K_d and $[L]_0$. The above data points were simulated to illustrate the range where simultaneously fitting for K_d and $[L]_0$ produce accurate results. For each plot, the fit K_d value was set to 5 times greater than the true K_d value, and the fit $[L]_0$ value was chosen to minimize the error. The data points and the black lines represent the true K_d and $[L]_0$ values for each plot. (a) Within the optimal range for accurate K_d and $[L]_0$, measurement by simultaneous fitting ($T_H > K_d > 0.1 \times T_L$, obtained from Figures 2e and 2f), the erroneously fit K_d and $[L]_0$ (red dashed lines) do not match the data. However, when using a single target concentration (panel b) or working outside the appropriate target concentration ranges (panels c and d), plots using the erroneous values (red dashed lines) can show good overlap with the data, despite a 5-fold deviation in K_d.

Treating Antibodies as Divalent Ligands. Antibodies are divalent with two chemically equivalent target-binding sites. Most analysis model antibody binding by considering each antibody molecule as two separate ligands, each with a single identical binding site.[7] This approach poorly represents the true situation, because binding of the second target often has a weaker K_d value than the first, likely due to a combination of effects such as excluded volume from binding the first target molecule.[25−27] Using the reverse assay to derive quantitative data has also been problematic, because of inadequate consideration of avidity issues, where many times the measured parameters can be more indicative of the experimental conditions than the ligand kinetics.[10] This is unfortunate

DOI: 10.1021/acs.analchem.5b03069
Anal. Chem. 2015, 87, 11755−11762

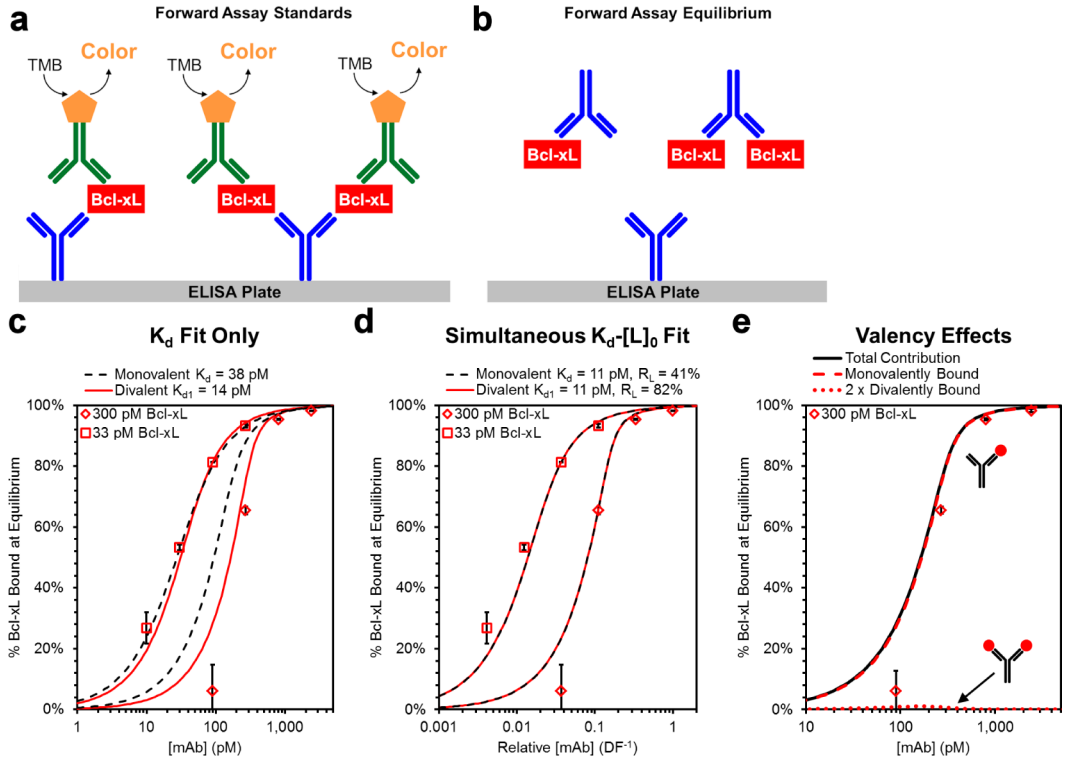

Figure 4. In the forward assay, accurate K_d and $[L]_0$ values can be determined by modeling antibodies as monovalent ligands. (a) Schematic to generate the standard curve for the forward assay. The target can bind to immobilized antibody on solid support (here, ELISA plate) in a monovalent or divalent format. (b) Schematic for the forward assay at equilibrium. Equilibration of target and antibody generates both monovalently bound and divalently bound target-ligand complexes. Neither complex can interact with the immobilized antibody on the solid support, lowering the signal similarly to Figure 1b. (c) The traditional approach to determine binding constants (a monovalent model using the number of antibody sites as the ligand concentration) results in both large errors and erroneous K_d values (dashed black lines) when fit for both target concentrations. A model treating the ligand as divalent results in better fits at both target concentrations (red lines). (d) Simultaneous fitting of K_d and $[L]_0$ results in excellent fits for both monovalent and divalent models and gives identical values for K_d, but results in a 2-fold difference in the fit ligand concentration (R_L is the ratio of the fit $[L]_0$ to known $[L]_0$). The K_d values from the simultaneous fits also match well with the divalent K_d-only fits in panel c. (e) Fraction of signal due to monovalent (red dashes) and divalent (red dots) antibody-target complexes. In the forward assay, >99% of the signal arises from the monovalent complex.

because the reverse assay is much more efficient at determining the K_d of one ligand vs many targets than the forward assay (e.g., to determine the specificity of a ligand). To address these issues, we systematically attempted to fit data in the forward and reverse assays with monovalent and explicit divalent models, toward the goal of quantifying valency effects and developing a useful version of the reverse assay.

Divalent Ligands: Forward Assay. The forward assay (Figure 4a and 4b) is the same for both monovalent and divalent ligands. When only fitting for K_d, the divalent model provides better fits for the data than the monovalent model (Figure 4c) and gives markedly different results for K_d (38 pM for the monovalent model vs 14 pM for the divalent model). When fitting for both K_d and $[L]_0$ simultaneously (Figure 4d), both models give curves that fit the data well and produce K_d values identical to the divalent K_d-only fit (K_d = 11 pM). However, the monovalent model produces a fit $[L]_0$ that is equivalent to the antibody concentration and thus half of the total concentration of sites. Our data indicate that, for the forward assay to give accurate K_d values, one must use the antibody concentration (rather than the number of sites) with the monovalent equilibrium model, a marked change from current practice. This is due to the negligible contribution of the divalently bound ligand at equilibrium for the forward assay (Figure 5e), essentially turning antibodies into monovalent ligands under these conditions.

In the first part of this paper, we showed how a pair of erroneous K_d and $[L]_0$ values can match the data points when a single target concentration is used. Since most equilibrium immunoassays to determine antibody K_d values use a single target concentration, previous studies have failed to uncover this discrepancy. This issue is only observed when multiple target concentrations are used; however, it is often simply attributed to ligand activity. An activity coefficient of 0.5 is often obtained, arguing that half of antibody sites are nonfunctional (i.e., mean activity coefficient for various antibodies, reported as 0.47 ± 0.07 (ref 22) and 0.53 ± 0.05 (ref 23)).

Divalent Ligands: Reverse Assay. Schematics for the reverse assay are shown in Figures 5a and 5b. Unlike that observed in the forward assay, in the reverse assay, the target is immobilized and used to capture the free ligand in solution (Figure 5a). The main difference between the forward assay and the reverse assay is that for multivalent ligands, monovalently bound ligands are still able to interact with the immobilized target (Figure 5b). The strength of this interaction is dependent on the cooperativity of the binding sites, as well as the immobilized target density. Because of this effect, the use of the reverse assay has been discouraged in the past.[11] For the

DOI: 10.1021/acs.analchem.5b03069
Anal. Chem. 2015, 87, 11755−11762

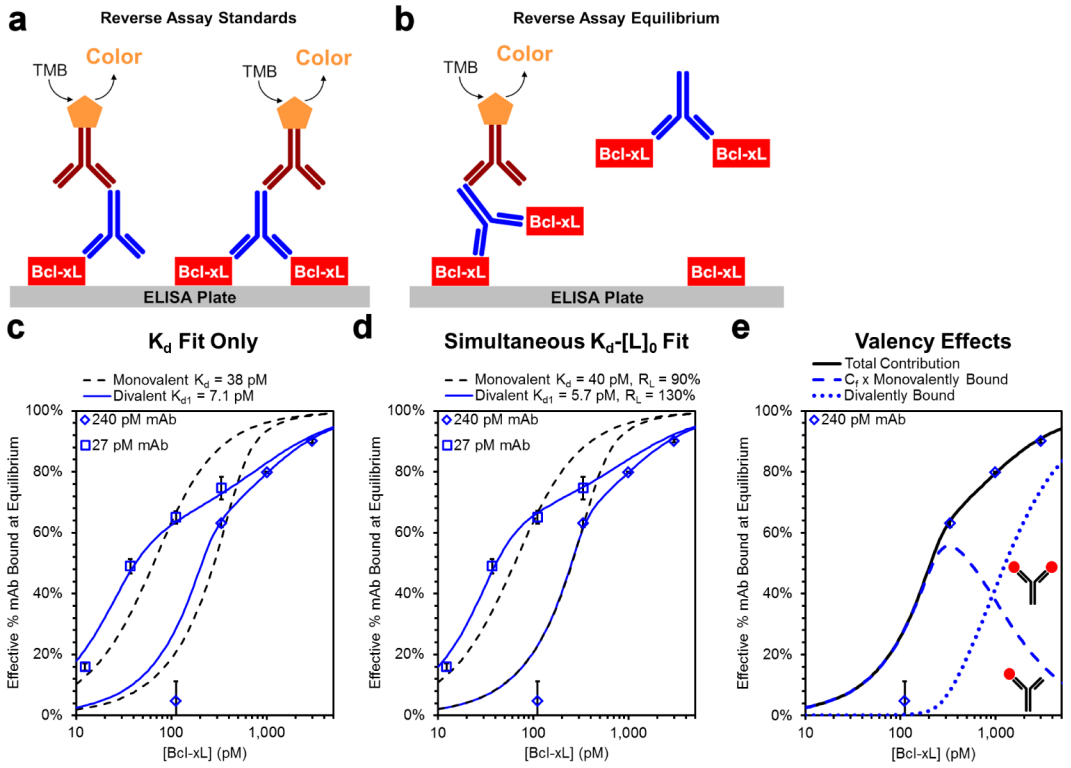

Figure 5. In the reverse assay (target-immobilized), determination of K_d and $[L]_0$ can only be done accurately when a divalent model is used. (a) Schematic to generate the standard curve for the reverse assay. The antibody can bind to a single immobilized target on solid support or it can bridge two nearby target proteins. (b) Schematic for the reverse assay at equilibrium. The monovalently bound ligand can bind to the immobilized target and give rise to signal whereas the divalently bound ligand cannot. (c) Calculating the K_d values for the reverse immunoassays. The best-fit curve of the monovalent equilibrium model does not match the experimental data for either high (blue diamonds) or low (blue squares) ligand concentration sets. In contrast, the divalent model (solid line) matches the data very closely. (d) Simultaneous fitting of K_d and $[L]_0$ for the reverse assay. The monovalent model does not match the data when K_d and $[L]_0$ are fit simultaneously. Both the divalent and the monovalent K_d values are similar to the calculated values in panel c. (e) The divalent complex has a very significant contribution in the reverse assay. At low target concentrations, the monovalent complex dominates the signal, whereas at high target concentrations, the divalent complex has a greater contribution. This effect can be treated using a negative cooperativity term (C_f) corresponding to the percent of monovalently bound ligand that does not interact with the immobilized target.

divalent equilibrium model, we added a cooperativity term to account for the strength of interaction between the target and a free ligand versus a monovalently bound ligand. The cooperativity factor (C_f) measures the percentage of the monovalently bound ligand that does not interact with the immobilized target. This means that, for the divalent model, the effective complex concentration at equilibrium is the concentration of the divalently bound ligand (unable to interact with the immobilized target) plus the concentration of the monovalently bound ligand multiplied by the cooperativity factor C_f (which represents the concentration of the monovalently ligand that is unable to interact with an immobilized target).

Similar to the forward assay, two concentrations of the species in solution (here, the monoclonal antibody) were used to obtain accurate K_d and $[L]_0$ values. Data from a sample reverse assay is shown in Figure 5c. When the high and low ligand concentrations are fit to equilibrium models, only the divalent model simulates the behavior of the obtained data points. Interestingly, simultaneously fitting for both K_d and $[L]_0$ does not help the monovalent model match the data better than fitting for K_d only (Figure 5d). For the reverse assay, both the monovalently bound and divalently bound species are present at significant quantities and contribute to the effective complex composition at equilibrium. Although, at low target concentrations, the monovalently bound ligand dominates the signal, at high target concentration the divalently bound ligand has the most significant contribution (Figure 5e). The value of C_f is dependent on several factors, such as K_{d1}, K_{d2}, and immobilized target density. The value of the cooperativity factor was obtained by fitting and remained consistent for all experiments: C_f = 74% ± 4% for the K_d-only fit and C_f = 73% ± 3% for the simultaneous K_d−$[L]_0$ fit.

CONCLUSIONS

We have developed an approach to determine both K_d and $[L]_0$ values for a ligand−target interaction simultaneously. We demonstrate the method with two assay platforms (Acoustic Membrane MicroParticle (AMMP) and Enzyme-Linked Immunosorbant Assay (ELISA)) and three classes of ligands (peptides, small molecules, and antibodies). The indication is that the approach will be general to other assay systems as well. The K_d and $[L]_0$ values are obtained by performing quantitative equilibrium immunoassays with two different concentrations of target and fitting the data simultaneously to the equilibrium model. We tested the validity of our approach vigorously by performing detailed error analysis, and we demonstrate that our fitting gives unique and reproducible solutions. Furthermore, we defined where K_d and $[L]_0$ measures are reliable and where they are underdetermined. By using a divalent equilibrium

DOI: 10.1021/acs.analchem.5b03069
Anal. Chem. 2015, 87, 11755−11762

model for antibody binding, we have shown that obtaining reliable K_d and $[L]_0$ values is only possible when the cooperativity factor between the two antibody binding sites has been taken into account. This approach solves a long-term problem of obtaining quantitative data from reverse assays.

■ ASSOCIATED CONTENT

Supporting Information

The Supporting Information is available free of charge on the ACS Publications website at DOI: 10.1021/acs.analchem.5b03069.

Details about the methods used for protein expression and purification, peptide synthesis, radiolabeled off-rate assay, bead loading, fluorescein labeling of the anti-HIS and anti-rabbit antibodies, sample preparation, ELISA assays, and AMMP assays (PDF)

■ AUTHOR INFORMATION

Corresponding Author

*Address: 3710 McClintock Ave., RTH-507, Los Angeles, CA, 90089-2905, USA. Tel.: 213-821-4250. E-mail: richrob@usc.edu

Notes

The authors declare no competing financial interest.

■ ACKNOWLEDGMENTS

This work was supported by NIH (Grant Nos. R01AI085583 (to R.W.R.) and R01CA170820 (to R.W.R. and T.T.T.) and the Ming Hsieh Institute for Research on Engineering−Medicine for Cancer (to R.W.R.). We thank Brett Masters (BioScale, Inc.) for discussions of data and experimental design, and BioScale, Inc. for providing access to the ViBE BioAnalyzer and the universal detection cartridges used in these experiments.

■ REFERENCES

(1) *Nat. Methods* **2015**, *12*, 373 (Editorial).10.1038/nmeth.3397

(2) Landry, J. P.; Ke, Y.; Yu, G. L.; Zhu, X. D. *J. Immunol. Methods* **2015**, *417*, 86−96.

(3) Bradbury, A.; Pluckthun, A. *Nature* **2015**, *518*, 27−29.

(4) Thakkar, S.; Nanaware-Kharade, N.; Celikel, R.; Peterson, E. C.; Varughese, K. I. *Sci. Rep.* **2014**, *4*, 3673.

(5) McGhee, J. D.; von Hippel, P. H. *J. Mol. Biol.* **1974**, *86*, 469−489.

(6) Fried, M.; Crothers, D. M. *Nucleic Acids Res.* **1981**, *9*, 6505−6525.

(7) Friguet, B.; Chaffotte, A. F.; Djavadi-Ohaniance, L.; Goldberg, M. E. *J. Immunol. Methods* **1985**, *77*, 305−319.

(8) Luo, L.; Luo, Q.; Guo, L.; Lv, M.; Lin, Z.; Geng, J.; Li, X.; Li, Y.; Shen, B.; Qiao, C.; Feng, J. *J. Biomol. Struct. Dyn.* **2014**, *32*, 416−423.

(9) Hakimi, H.; Nguyen, T. T.; Suganuma, K.; Masuda-Suganuma, H.; Angeles, J. M.; Inoue, N.; Kawazu, S. *Trop. Med. Health* **2013**, *41*, 55−59.

(10) Kaufman, E. N.; Jain, R. K. *Cancer Res.* **1992**, *52*, 4157−4167.

(11) Rich, R. L.; Myszka, D. G. *J. Mol. Recognit.* **2007**, *20*, 300−366.

(12) Fei, Y.; Sun, Y. S.; Li, Y.; Lau, K.; Yu, H.; Chokhawala, H. A.; Huang, S.; Landry, J. P.; Chen, X.; Zhu, X. *Mol. BioSyst.* **2011**, *7*, 3343−3352.

(13) Sun, Y. S.; Landry, J. P.; Fei, Y. Y.; Zhu, X. D.; Luo, J. T.; Wang, X. B.; Lam, K. S. *Langmuir* **2008**, *24*, 13399−13405.

(14) Blake, R. C., 2nd; Li, X.; Yu, H.; Blake, D. A. *Biochemistry* **2007**, *46*, 1573−1586.

(15) Boise, L. H.; Gonzalez-Garcia, M.; Postema, C. E.; Ding, L.; Lindsten, T.; Turka, L. A.; Mao, X.; Nunez, G.; Thompson, C. B. *Cell* **1993**, *74*, 597−608.

(16) Oltersdorf, T.; Elmore, S. W.; Shoemaker, A. R.; Armstrong, R. C.; Augeri, D. J.; Belli, B. A.; Bruncko, M.; Deckwerth, T. L.; Dinges, J.; Hajduk, P. J.; Joseph, M. K.; Kitada, S.; Korsmeyer, S. J.; Kunzer, A. R.; Letai, A.; Li, C.; Mitten, M. J.; Nettesheim, D. G.; Ng, S.; Nimmer, P. M.; O'Connor, J. M.; Oleksijew, A.; Petros, A. M.; Reed, J. C.; Shen, W.; Tahir, S. K.; Thompson, C. B.; Tomaselli, K. J.; Wang, B.; Wendt, M. D.; Zhang, H.; Fesik, S. W.; Rosenberg, S. H. *Nature* **2005**, *435*, 677−681.

(17) O'Connor, L.; Strasser, A.; O'Reilly, L. A.; Hausmann, G.; Adams, J. M.; Cory, S.; Huang, D. C. *EMBO J.* **1998**, *17*, 384−395.

(18) Sleebs, B. E.; Kersten, W. J.; Kulasegaram, S.; Nikolakopoulos, G.; Hatzis, E.; Moss, R. M.; Parisot, J. P.; Yang, H.; Czabotar, P. E.; Fairlie, W. D.; Lee, E. F.; Adams, J. M.; Chen, L.; van Delft, M. F.; Lowes, K. N.; Wei, A.; Huang, D. C.; Colman, P. M.; Street, I. P.; Baell, J. B.; Watson, K.; Lessene, G. *J. Med. Chem.* **2013**, *56*, 5514−5540.

(19) Jalali-Yazdi, F.; Corbin, J. M.; Takahashi, T. T.; Roberts, R. W. *Anal. Chem.* **2014**, *86*, 4715−4722.

(20) Xie, L.; Mark Jones, R.; Glass, T. R.; Navoa, R.; Wang, Y.; Grace, M. J. *J. Immunol. Methods* **2005**, *304*, 1−14.

(21) Rathanaswami, P.; Richmond, K.; Manchulenko, K.; Foltz, I. N. *Anal. Biochem.* **2011**, *414*, 7−13.

(22) Bee, C.; Abdiche, Y. N.; Stone, D. M.; Collier, S.; Lindquist, K. C.; Pinkerton, A. C.; Pons, J.; Rajpal, A. *PLoS One* **2012**, *7*, e36261.

(23) Bee, C.; Abdiche, Y. N.; Pons, J.; Rajpal, A. *PLoS One* **2013**, *8*, e80501.

(24) Darling, R. J.; Brault, P. A. *Assay Drug Dev. Technol.* **2004**, *2*, 647−657.

(25) Harms, B. D.; Kearns, J. D.; Iadevaia, S.; Lugovskoy, A. A. *Methods* **2014**, *65*, 95−104.

(26) Krishnamurthy, V. M.; Estroff, L. A.; Whitesides, G. M. In *Fragment-Based Approaches in Drug Discovery*; Wiley−VCH Verlag GmbH & Co. KGaA: Weinheim, Germany, 2006; pp 11−53.

(27) Mack, E. T.; Snyder, P. W.; Perez-Castillejos, R.; Whitesides, G. M. *J. Am. Chem. Soc.* **2011**, *133*, 11701−11715.

DOI: 10.1021/acs.analchem.5b03069
Anal. Chem. 2015, 87, 11755−11762